

Epigenetic-modification associated hnRNPA3 acts as a prognostic biomarker and promotes malignant progression of HCC

Xufan Cai

Zhejiang Provincial People's Hospital, Hangzhou Medical College

Weihui Guo

Zhejiang Provincial People's Hospital, Hangzhou Medical College

Fang Wu

Zhejiang Provincial People's Hospital, The Affiliated People's Hospital of Hangzhou Medical College

Weilang Xu

Zhejiang Provincial People's Hospital, Hangzhou Medical College

Tao Ding

Zhejiang Provincial People's Hospital, Hangzhou Medical College

Yizhe Diao

Zhejiang Provincial People's Hospital, Hangzhou Medical College

Lei Wang

Zhejiang Provincial People's Hospital, Hangzhou Medical College

Zhenyuan Qian

Zhejiang Provincial People's Hospital, The Affiliated People's Hospital of Hangzhou Medical College

Guangyuan Song

11718244@zju.edu.cn

Zhejiang Provincial People's Hospital, The Affiliated People's Hospital of Hangzhou Medical College

Research Article

Keywords: hnRNPA3, HCC, DNA methylation, immune infiltration, ceRNA, drug sensitivity

Posted Date: December 24th, 2024

DOI: <https://doi.org/10.21203/rs.3.rs-5662447/v1>

License:  This work is licensed under a Creative Commons Attribution 4.0 International License.

[Read Full License](#)

Additional Declarations: No competing interests reported.

Abstract

Objective

hnRNPA3 is highly expressed in numerous malignancies, including hepatocellular carcinoma (HCC), but its function and mechanism has not been elucidated. In this study, we performed a comprehensive bioinformatics analysis of hnRNPA3 in the TCGA-LIHC dataset and several experiments in vitro to investigate the function and potential mechanisms of hnRNPA3 in HCC.

Methods

Pan-cancer expression including hnRNPA3 levels as well as DNA methylation, associated ceRNA, immune infiltration, and immune checkpoint genes of hnRNPA3 in TCGA-LIHC dataset were assessed. Logistic regression, receiver operating characteristic curve (ROC), Kaplan-Meier analysis, and nomogram modeling were used to evaluate prognostic values of hnRNPA3 in HCC. hnRNPA3 level in cell subtypes in HCC tumor microenvironment was analysed through spatial transcriptomic. “pRRophetic” package was used to predict potential chemotherapeutic drugs sensitivity. hnRNPA3 level in HCC patients and cell lines were detected by qRT-PCR or WB. hnRNPA3’s impact on proliferation, migration were studied in SNU449 and HuH7 cell lines. RNA-seq showed hnRNPA3 controlled different important signaling pathways in HCC.

Results

hnRNPA3 was significantly elevated in HCC tumors compared to controls. hnRNPA3 levels correlated with Age, HCC stage, histologic grade, and tumor status, and may independently predict the overall and disease-specific survival. Significant associations were found between hnRNPA3 levels and DNA methylation. hsa-miR-22-3p may act as a regulatory factor for hnRNPA3 and form a ceRNA network with multiple lncRNAs. Analysis of immune infiltration and immune checkpoint genes revealed a correlation between hnRNPA3 expression and macrophages. The similar conclusion also occurred in the spatial transcriptomic detection. 5-Fluorouracil, Doxorubicin, Etoposide, et al, may be potential sensitive drugs in therapy of high-hnRNPA3 HCC patients. Silencing hnRNPA3 expression in SNU449 and HuH7 cells resulted in reducing proliferation and migration. RNA-seq showed hnRNPA3 played an important regulatory role in the malignant progression of HCC.

Conclusion

hnRNPA3 was found to represent a promising biomarker within HCC diagnosis and prognosis and maybe a potential drug-target in HCC therapy.

Introduction

Hepatocellular carcinoma (HCC), the most common primary liver cancer, is the sixth most common cancer and the third most common cause of cancer-related deaths worldwide¹. Although some of patients are cured by local hepatectomy, the overall survival outcome of HCC is still poor. The bad prognosis can be attributed to that a big number of patients were diagnosed with advanced disease. Therefore, improving survival rates, early detection and discovering the potential therapeutic drugs of HCC is crucial.

Heterogeneous nuclear ribonucleoproteins (hnRNPs) are a large family of RNA-binding proteins. hnRNPA3 is a member of the hnRNPA/B family, encoded in humans by the hnRNPA3 gene. hnRNPA3s have been implicated in crucial tumor progression processes including proliferation and apoptosis^{2,3}. For example, hnRNPA3 is involved in RNA binding, mRNA transport and mRNA splicing via spliceosome. hnRNPA3 may increase the expression of APOBEC3B, a vital cytosine deaminase in cancer cell line through mRNA splicing via spliceosome.⁴ In NSCLC, hnRNPA3 can antagonize the expression of alternative splicing factor/splicing factor 2 (ASF/SF2)⁵. In HCC, hnRNPA3 combined with glypican 3 (GPC3) performed well in differential diagnosis between high-grade dysplastic nodule (HGDN) and early HCC. Furthermore, high expression of hnRNPA3 was found to be associated with poor survival rates in HCC patients⁶. However, the function of hnRNPA3 in HCC and the mechanism remains unknown.

DNA methylation, as one of the important mechanisms of epigenetic regulation, has profound effects on gene expression, genome stability, and various biological processes⁷. DNA methylation is mainly regulated by DNA methyltransferases and DNA demethylases. DNA methyltransferases, mainly containing DNMT1, DNMT3a, DNMT3b and DNMT3L, may increase the DNA methylation level and lead to the decreased expression of regulated genes. On the contrary, DNA demethylases, mainly including TET1, TET2, TET3, will reduce the methylation level and result in the upregulation of associated genes^{8,9}.

microRNAs (miRNAs) and long non-coding RNAs (lncRNAs) are two important non-coding RNAs that play key regulatory roles in tumor progression^{10,11}. There exists a mutual regulatory relationship between miRNA and lncRNA. lncRNA can act as a competitive endogenous RNA (ceRNA) to interact with miRNA, participating in the expression regulation of target genes. Conversely, miRNA can also regulate lncRNA through the RNA-induced silencing complex (RISC) to exert biological functions. This mutual regulatory relationship plays a crucial role in the occurrence and progression of various diseases, providing new targets and research ideas for disease treatment.

In this study, through comprehensive bioinformatics, we found epigenetic regulations (DNA methylation and ceRNA) played a vital role in the abnormal expression of hnRNPA3. Spatial transcriptomics revealed hnRNPA3 was closely related to macrophage, which may lead to the malignant progression of HCC. Besides, we also found hnRNPA3 may accurately predict the 1, 3, 5 years survival of HCC patients. hnRNPA3 also can prompt the proliferation, migration and invasion of HCC. Pharmacological analysis proved that lower hnRNPA3 may have a better result due to the lower IC₅₀ of many anti-tumor drugs. All

in all, hnRNPA3 may be a promising biomarker within HCC diagnosis and prognosis and maybe a potential drug-target in HCC therapy.

Materials and Methods

1. Patients and specimens

A total of 36 pairs of human HCC tissues and matched normal tissues were collected from Zhejiang Provincial People's Hospital. All specimens were obtained from patients who were clinically and histopathologically diagnosed with HCC, who did not receive radiotherapy or chemotherapy treatment before surgery. Tissues were snap-frozen and placed in a -80 °C refrigerator. Written consents were obtained from all patients before participation in the study. The study was approved by the medical ethics committee of Zhejiang Provincial People's Hospital.

2. Gene expression profile of hnRNPA3 in pan-cancer

The RNA sequencing data of hnRNPA3 across 33 types tumor patients were obtained from The Cancer Genome Atlas (TCGA, <https://portal.gdc.cancer.gov/>) and the hnRNPA3 expression across 33 types tumor patients were analysed in TIMER (<https://cistrome.shinyapps.io/timer/>) .

3. hnRNPA3 expression in GSE76427

The expression of hnRNPA3 expression in GSE76427 was download from the Gene Expression Omnibus (GEO, <https://www.ncbi.nlm.nih.gov/geo/>) and analysed with R Studio.

4. Clinical relationship of hnRNPA3 in HCC

The related TCGA-LIHC clinicopathological information were obtained from TCGA and were analysed through R studio.

5. Prognostic evaluation of hnRNPA3 in HCC

For survival analysis, we employed the online platform kmplot (<https://www.kmplot.com/>) to evaluate and plot the performance of hnRNPA3 in overall survival (OS), disease-free survival (DFS), progression-free survival (PFS), and relapse-free survival (RFS). Receiver operating characteristic curve (ROC) curve of 1,3,5 years survival was plot through R studio. Univariate Cox regression analysis,multivariate Cox regression analysis and nomogram modeling were established to evaluate the prognostic value of hnRNPA3 in HCC in R studio with "forestplot", "rms" packages.

6. Relationship between HNRNPA3 expression and DNA methylation in HCC

We obtained the methylation value of hnRNPA3 across 33 tumors in TCGA and the differential methylation site from SMATR (<http://www.bioinfo-zs.com/smartapp/>). We also plotted the survival curve

of differential methylation site in SMART. The combined survival of hnRNPA3 and DNA methylases or demethylases were finished by using R studio with “survival” package.

7. Immunoinfiltration analysis of HNRNPA3

TIMER (<https://cistrome.shinyapps.io/timer/>) is a free online platform offering a suite of tools, including six distinct computational methods to estimate immune cell infiltration levels, and to investigate the correlations between immune infiltration and gene expression, mutations, and survival traits within the TCGA dataset¹². Utilizing TIMER, we produced a correlation map that delineates the inter relationships between various immune cell types and the hnRNPA3 in hepatocellular carcinoma. We employed the Corrplot R package to visualize the correlation between hnRNPA3 and immune checkpoint-related genes in TCGA-LIHC.

The Cancer Immunome Atlas (TCIA, <https://tcia.at/home>) encompasses T-cell receptor (TCR) and B-cell receptor (BCR) sequencing data, along with details on immune cell types, phenotypes, functions, and interactions, which aids in the development of novel cancer immunotherapy strategies¹³. We retrieved the hepatocellular carcinoma-related immunophenotype score (IPS) from TCIA and compared the results based on the median expression levels of hnRNPA3.

8. The ceRNA network for hnRNPA3 in HCC

Starbase (<http://starbase.sysu.edu.cn/>) was used to acquire potentially related miRNAs and lncRNAs of hnRNPA3. And we described a ceRNA for hnRNPA3 in HCC.

9. Spatial transcriptome analysis

We interfaced with the Sparkle database (<https://grswsci.top/>) and the SpatialTME platform (<https://www.spatialtme.yelab.site/>) to carry out a LIHC spatial transcriptomic analysis. Spatial transcriptomic data from a previous study (PMID: 36708811) were used. The Cottrazm package was instrumental in deconvoluting the cellular constituents of the tumor microenvironment (TME) through the `get_enrichment_matrix` and `enrichment_analysis` functions, which were pivotal in constructing an enrichment matrix for various cell types¹⁴. Visualization of the predominant cell types within each microregion was achieved using the `SpatialFeaturePlot` function from the Seurat package¹⁵. This function also facilitated the depiction of the spatial landscape of HNRNPA3 expression across individual spots. Spots were designated as ‘Mal’ if the malignancy score was 1, indicating the presence of malignant cells, and as ‘nMal’ if the score was 0, indicating their absence. Spearman correlation analysis was employed to compute the correlations between cellular composition and gene expression levels across all spots, with visualization facilitated by the linkET package.

10. Drug sensitivity prediction

The R package “pRRophetic” trains and constructs models for predicting chemotherapy response using the cgp2016 cell line data¹⁶. The Wilcoxon signed-rank test was employed to assess differences in IC50

values across the two groups. By comparing the drug sensitivities between the two groups with high and low expression of hnRNPA3, drugs with a p-value less than 0.001 are considered to have a potential association with hnRNPA3.

11. Cell culture

Immortalized liver cell line Li5 was presented with The First Affiliated Hospital of Zhejiang University School of Medicine. Human HCC cell lines SNU449, Huh7, HepG2, Hep3B2.1-7, PLC/PRF/5, HCC97h, HCCLM3, HepG2.2.15, and HLE were obtained from ATCC. They were cultured in DMEM with 10% FBS contained. All cell lines were cultured in the indicated humidified environment (37 °C, 5% CO₂).

11. RNA extraction and qRT-PCR

FastPure Cell/Tissue Total RNA Isolation Kit V2 (Vazyme Biotech Co., Ltd, Nanjing, China) was employed for the total RNA extraction, and HiScriptIII RT SuperMix for qPCR (+gDNA wiper) (Vazyme Biotech Co., Ltd, Nanjing, China) was used to cDNA synthesis. The qRT-PCR was constructed based on SYBR Green Mix (Vazyme Biotech Co., Ltd, Nanjing, China) in a total 20 µl of volume and performed on Applied Biosystems® 7500 Real - Time PCR System. The relative expression was calculated with $2^{-\Delta\Delta CT}$. The primers were designed and produced by Repobio (Hangzhou, China):

hnRNPA3-qF:ACGTTCCAGGGGCTTTGGT; hnRNPA3-qR:TGGTTCCACTACACGCCCA

12. Western Blot(WB)

RIPA/ protease inhibition mixture was added into cells or tissues to obtain protein lysates. Using BCA kit (Vazyme Biotech Co.,Ltd,Nanjing,China) to detect the protein concentration. Total proteins were separated by SDS-PAGE, transferred to PVDF membranes, and closed with rapid closure solution (ABclonal Wuhan China). After incubation with primary antibody overnight at 4°C, the corresponding secondary antibody was added to membranes and incubated for 1 h at room temperature. Finally, membranes were incubated using the ECL Chemiluminescence Kit in the gel imaging system (BIO-RAD) exposure and development. Blot images were analyzed with ImageJ. The information of antibodies were as follows:hnRNPA3 (1:1000, ABclonal, Wuhan, China),GAPDH (1:100000, ABclonal, Wuhan, China)

13. Lentivirus infection

A lentiviral hnRNPA3 stable silencing vector and its control lentivirus were constructed by GeneChem (Shanghai, China) and used to infect HCC cell lines SNU449 and Huh7. Puromycin was used to screen positive cells. The infection efficiency was verified by observing fluorescence intensity in fluorescence microscopy and detecting expression of proteins with WB. The shRNA sequence was as follows: sh-hnRNPA3: AGGTGATGGTGGATATAAT.

14. Cell proliferation assays.

CCK-8 assays were performed to examine the effect of silencing HNRNPA3 in SNU449 and Huh7. Two types of cells were seed in 96-well plates (2000 cells per well). After 0h,24h,48h,72h, CCK-8 solution added for 1 hour's incubation. The absorbance was subsequently measured at 450 nm.

15. Colony formation assay

SNU449 and Huh7 after successful stable silencing were seeded in 6-well plates (1000 cells per well) and incubated for 14 days. Then the cell colonies fixed and stained with 4% polymethylene and 1% crystal violet. The cell colonies were observed and photographed under a microscope.

16. Cell migration and invasion assays

Transwell assays were used to examined cells migration and invasion. In short, 80000 of cells were suspended and seeded into the transwell upper chambers (inserted 8.0μM of PET membranes). The chambers with cell suspensions were placed in 24-well plates with 20% FBS-containing DMEM (500 μL per well) added. After incubating 24 h,4% polymethylene was used to fixed those lower chambers of cells followed by 1%crystal violet staining. Finally, the stained cells were observed and photographed based on at least three randomly selected fields under a microscope. For invasion assay, the membrane needed to be pre-coated with

Matrigel in advance, and the rest of the steps were the same as above.

Scratch test is a another assay to examine cells migration. Cells were seed into a 6-well plate and incubated to reach confluence. The monolayer was scratched using a tip and the cells were cultured in serum-free medium. Migration areas were photographed at 0 h, 12 h and 24 h later under a microscope.

17. RNA-seq

The total RNA of SNU449 cells was extracted after stable silencing HNRNPA3, and then RNA-seq was conducted by Cosmos Wisdom Biotech Co., Ltd (Hangzhou, China) to screen differentially expressed genes (DEGs). R version 3.6.3 and R version 4.1.3 were utilized respectively for the heatmap and the volcano plot. GO and KEGG enrichment analyses were performed by DAVID Bioinformatics Resources (<https://david.ncifcrf.gov/>).

18. Statistic analysis

GraphPad prism 9.0 was adopted for analyzing the data, which were stated as mean ± SD, by t-test or oneway ANOVA. A P value less than 0.05 was defined there is a significant difference.

Results

1.hnRNPA3 is highly expressed in HCC and asociated with HCC patients' prognosis.

Firstly, we investigated the expression level of hnRNPA3 across various cancers and found that hnRNPA3 is significantly high expressed in numerous tumor types, liver hepatocellular carcinoma (LIHC), breast cancer (BRCA), cholangiocarcinoma (CHOL), colorectal adenocarcinoma (COAD), and including bladder cancer (BLCA), among others (Fig. 1A). Subsequent analysis revealed that hnRNPA3 expression correlates with Age, Gender, Grade, Stage (Fig. 1B). Additionally, in TCGA-LIHC and the GSE76427, we observed a significant upregulation of hnRNPA3 in tumor samples compared to normal tissue samples (Fig. 1C). Interestingly, the cohort from Kaplan-Meier Plotter showed that higher hnRNPA3 expression is correlated with worse prognosis of HCC (DFS: HR = 2.22, 95% CI 1.21–4.07, P = 0.0081; OS: HR = 1.55, 95% CI 1.06–2.27, P = 0.023; PFS: HR = 1.66, 95% CI 1.2–2.31, P = 0.002; RFS: HR = 1.63, 95% CI 1.13–2.35, P = 0.008) (Fig. 1D-G). The prognostic capacity of hnRNPA3 was evaluated by using the area under the curve (AUC) of a ROC curve. The ROC curve analysis showed that the area which AUC at 1 year was 0.688, AUC at 2 years was 0.625 and AUC at 3 years was 0.565 (Fig. 1H).

2. hnRNPA3 acts as an indicator for survival prediction

To ascertain the independent prognostic significance of hnRNPA3 in hepatocellular carcinoma (HCC), we performed both univariate and multivariate Cox regression analyses on the TCGA dataset, utilizing the 'forestplot' R package for visualization. Both the univariate and multivariate analysis indicated a strong association between hnRNPA3 expression, stage, and patient prognosis within the TCGA dataset (Fig. 2A, 2B). For this investigation, we developed a nomogram model incorporating age, gender, tumor grade, stage, and hnRNPA3 expression levels as variables, facilitated by the 'rms' R package. This nomogram significantly enhanced the clinical utility in predicting 1-, 3-, and 5-year survival rates for HCC patients (Fig. 2C). The calibration curves for the TCGA cohort (Fig. 2D) demonstrated high predictive accuracy for the 1-, 3-, and 5-year OS of HCC patients, as indicated by the C-index. These findings confirm hnRNPA3 as a robust, independent prognostic indicator for HCC.

3. hnRNPA3 is related with DNA hypomethylation in HCC

In our epigenetic profiling study, we observed a significant hypomethylation of hnRNPA3 (Beta-value) across multiple cancer types, especially in LIHC (Fig. 3A). To delineate the underlying mechanisms, we investigated the correlation between hnRNPA3 and DNA methyltransferases and DNA demethylases, revealing significant associations with DNA methyltransferase 3-like (DNMT3L) ($r = -0.151$, $p = 3.59e-03$) and DNA demethylases, such as, ten-eleven translocation 1 (TET1) ($r = 0.647$, $p = 1.98e-45$), TET2 ($r = 0.555$, $p = 2.2e-31$), and TET3 ($r = 0.741$, $p = 8.09e-66$) (Fig. 3I-L). Corresponding to the above, survival analysis indicated that samples with high hnRNPA3 expression and low DNMT3L expression had a significantly worse prognosis compared to those with low HNRNPA3 and high DNMT3L expression ($p = 0.005$) (Fig. 3M). Conversely, samples with concurrent high expression of hnRNPA3 and TET1, TET2, and TET3 exhibited a favorable survival outcome compared to those with low expression of both HNRNPA3 and the TET family members (TET1, $p = 0.003$; TET2, $p = 0.015$; TET3, $p = 0.015$), suggesting that the methylation status of HNRNPA3 is a determinant in the prognostic landscape of HCC (Fig. 3.N-P).

Subsequent investigation identified cg11064170 as a CpG site with significantly reduced Beta-value in HCC tissues relative to normal tissue, implying a pivotal role for cg11064170 in the methylation process (Fig. 3B). A high degree of correlation was observed between cg11064170 methylation status and hnRNPA3 expression levels ($R = 0.42$, $p < 2.2e-16$), and significant differences in cg11064170 methylation were noted across different tumor stages ($p = 0.0047$) (Fig. 3C,D). Furthermore, in HCC, hypermethylation at cg11064170 was associated with a favorable disease-free interval ($p = 3e-04$), and Overall survival ($p = 0.0093$), contrarily, hypomethylation of cg01594915 and cg01750051 was indicative of better prognosis survival (cg01594915 in DFI, $p = 0.0272$; cg01750051, $p = 0.0018$) (Fig. 3M-P). These findings implicate cg11064170, cg01594915 and cg01750051 as critical regulatory factors in the methylation dynamics of hnRNPA3 in HCC.

4. Establishing the ceRNA regulatory network

In addition to DNA methylation, non-coding RNAs is also an important epigenetic modification. Utilizing the Starbase database, we identified multiple miRNAs potentially interacting with hnRNPA3 (Fig. 4A). Notably, hsa-miR-22-3p exhibited a significant inverse correlation with hnRNPA3 ($r = -0.34$, $p = 1.7e-11$) (Fig. 4B). Contrarily, hsa-miR-22-3p was found to be upregulated in normal tissue ($p = 2.2e-12$) (Fig. 4C) and its elevated expression was associated with improved overall survival ($p < 0.001$) (Fig. 4D), implying a tumor-suppressive role and suggesting that hsa-miR-22-3p may act as a regulatory factor for hnRNPA3.

Subsequent analysis revealed strong positive correlations between hnRNPA3 and several lncRNAs, including Z92544.1 ($r = 0.54$, $p < 2.2e-16$), SNHG16 ($r = 0.5$, $p < 2.2e-16$), SNHG14 ($r = 0.51$, $p < 2.2e-16$), SLC25A25-AS1 ($r = 0.45$, $p < 2.2e-16$), AL162431 ($r = 0.5$, $p < 2.2e-16$), AL008721 ($r = 0.47$, $p < 2.2e-16$), and AC008741 ($r = 0.43$, $p < 2.2e-16$), indicating potential involvement in the regulation of HNRNPA3 expression in HCC (Fig. 4E). To substantiate our hypothesis, we found that hsa-miR-22-3p also exhibited significant negative correlations with these lncRNAs: Z92544.1 ($r = -0.23$, $p = 6.8e-06$), SNHG16 ($r = -0.28$, $p = 6.8e-06$), SNHG14 ($r = -0.26$, $p = 3.5e-07$), SLC25A25-AS1 ($r = -0.25$, $p = 1.2e-06$), AL162431 ($r = -0.25$, $p = 7.4e-07$), AL008721 ($r = -0.22$, $p = 1.8e-05$), and AC008741 ($r = -0.24$, $p = 4.1e-08$) (Fig. 4F). High expression of these lncRNAs, except SLC25A25-AS1 ($p = 0.137$), in tumor tissues was indicative of a poorer prognosis (Fig. 4G-H), suggesting a role in disease progression. Lastly, based on the aforementioned analyses, we constructed the ceRNA regulatory network of hnRNPA3, elucidating the intricate interactions between hnRNPA3, miRNAs, and lncRNAs in HCC (Fig. 4I).

5. hnRNPA3 is associated with immunoinfiltration of HCC

To investigate the role of hnRNPA3 in the HCC immune microenvironment, TIMER analysis revealed significant correlations of HNRNPA3 with B cells ($r = 0.449$, $p = 1.87e-18$), CD8 + T cells ($r = 0.324$, $p = 8.55e-10$), CD4 + T cells ($r = 0.476$, $p = 7.89e-21$), macrophages ($r = 0.516$, $p = 1.31e-24$), neutrophils ($r = 0.497$, $p = 6.33e-23$), and dendritic cells ($r = 0.488$, $p = 9.90e-22$) (Fig. 5A). Subsequent studies suggest a robust correlation between HNRNPA3 and M2 macrophages ($r = 0.477$, $p = 4.77e-21$),

Macrophages_TIMER ($r = 0.427$, $p = 9.48e-17$) (Fig. 5B-C). Immuno-regulatory genes govern immune cell activity, proliferation, and function, impacting the tumor microenvironment and thereby influencing carcinogenesis, progression, and therapeutic outcomes. The Corrplot package was employed to illustrate correlations between hnRNPA3 and immunomodulatory genes, highlighting those with a correlation coefficient above 0.2 (Fig. 5D). Finally, the immune responsiveness of the groups was evaluated through IPS evaluation. The findings revealed that the scores for ips_ctla4_neg_pd1_neg were elevated in the group with low hnRNPA3 expression (Fig. 5E-H).

6. The spatial localization of hnRNPA3 within the spatial transcriptomic landscape.

Utilizing spatial transcriptomic technology, we integrated transcriptomic data with spatial information from hematoxylin and eosin (HE) stained sections. We quantified 3,382 and 4,142 spots in the P8T and P9T datasets, respectively, and calculated the cellular composition within each spot based on characteristic genes. This approach afforded us a direct visualization of the spatial expression relationships between various cell types and hnRNPA3 (Fig. 6A-H). In the tissue sections, we detected a significant overlap and positive correlation between the expression of hnRNPA3 and both tumor cells and macrophages (Fig. 5I, 5K). Furthermore, we noted that the expression of hnRNPA3 was markedly elevated in the malignant cell cohort (Mal) compared to the non-malignant cohort (nMal) (Fig. 5J, 5L). This spatial profiling suggests that hnRNPA3 is implicated in tumor progression and macrophage-associated immune processes. These findings are consistent with our results from the TIMER dataset.

7. Predicting potential chemotherapeutic or targeted-therapeutic drugs sensitive to hnRNPA3

To boost hnRNPA3's clinical utility in HCC, we utilized "pRRophetic" to forecast therapeutic response. We assessed the half-maximal inhibitory concentration (IC50) of standard therapies for HCC via the "pRRophetic" algorithm and analyzed IC50 differences between high and low hnRNPA3 expression groups. The results indicated that patients with low hnRNPA3 expression were more responsive to Erlotinib (Fig. 7C). Conversely, high hnRNPA3 patients showed greater sensitivity to 5-Fluorouracil, Doxorubicin, Etoposide, Gemcitabine, Imatinib, Lisitinib, Paclitaxel, Parthenolide, Rapamycin, Sunitinib, and Tipifarnib ($P < 0.001$) (Fig. 7A-B, D-L).

8. hnRNPA3 regulated proliferation and migration of HCC cells

In order to verify the expression of hnRNPA3 in HCC, qRT-PCR was used to detect the mRNA expression of hnRNPA3 in tumor tissues ($n = 36$) and matched adjacent normal tissues ($n = 36$) from the Zhejiang Provincial People's Hospital. It was shown that the mRNA expression of hnRNPA3 in tumor tissues was upregulated compared to that in matched normal tissues (Fig. 8A). The protein levels of several paired samples could be found the same result (Fig. 8B). In addition, nine HCC cell lines showed higher hnRNPA3 protein expression compared to Li5 cell lines, in particular for SNU449 and Huh7 (Fig. 8C). To further investigate the role of hnRNPA3 in HCC, hnRNPA3 was stably silenced in SNU449 and Huh7 cells,

with the efficiency of knockdown verified by WB (Fig. 8D). CCK-8 and colony formation assays indicated markedly reduced viability and proliferation of cells after hnRNPA3 knockdown (Fig. 8E-H). Transwell and scratch experiments were performed to examine cell invasion and migration, revealing a significant reduction in the migration abilities of SNU449 and Huh7 cells after hnRNPA3 knockdown (Fig. 8I-M). Draw a conclusion, these results suggested the involvement of hnRNPA3 in both cell proliferation and migration.

9. hnRNPA3 induced some important biological processes in HCC

To further investigate the underlying mechanism of hnRNPA3 functions, we performed RNA-seq in SNU449 cells with or without knockdown hnRNPA3 to detect DEGs. The sequencing outcomes told us that the agent led to 114 up-regulated and 331 down-regulated genes (Fig. 9A-C). Furthermore, enrichment analyses underscored the RAP1, MAPK, PI3K/Akt signaling pathway, and the biological processes like cell adhesion, signal transduction, and the regulation of cell proliferation (Fig. 9D-E).

Discussion

Despite the rapid development of diagnosis and treatment, the overall survival outcome of liver cancer is still poor. So, it is of great significance to explore more scientific and effective biomarkers and treatment strategies in HCC.

hnRNPs are defined as nuclear RNA-binding proteins that form complexes with pre-mRNA.

HnRNPs are located at the border regions of chromatin to interact with newly synthesized nuclear RNAs¹⁷. In human, hnRNPA3 is located on chromosome 2, as a biological role in the stable maintenance of telomere repeats¹⁸. A study revealed that the expression of hnRNPA3 increased in a stepwise manner from non-tumor cirrhotic tissue to DN and was the highest in HCC⁶. Although the hnRNPA3 is closely associated with cancer regulation, the information regarding hnRNPA3 within HCC is still limited.

Therefore, a comprehensive bioinformatics-based analysis was conducted to explore its possible functional and diagnostic roles in HCC. We observe a novel upsurge of hnRNPA3 expression in most cancers, notably in HCC, relative to normal tissue. And it was associated with tumor status and pathological phase, as well as survival outcomes. In addition, higher level of hnRNPA3 expression were related to worse patient prognosis and more advanced clinical stages of the tumor. These results were consistent with published articles in other cancers¹⁹⁻²². Furthermore, through univariate and multivariate analyses, we incorporated the clinicopathological features and risk score to enhance hnRNPA3's predictive performance power with developing a nomogram. The developed nomogram shows promising results in using hnRNPA3 to predict the HCC prognosis.

DNA methylation, an important epigenetic modification, affects the development of tumors in a variety of ways²³⁻²⁵. The occurrence and development of tumors are affecting by up-regulating or down-regulating

the DNA methylation level of the target gene²⁶. Here, we investigate and reveal that hnRNPA3 exhibits a lower methylation level in HCC tissues compared to normal tissue, which is inversely correlated with the expression level of hnRNPA3. Further investigation demonstrates a significant association between hnRNPA3 and the methylation regulatory proteins DNMT3L, TET1, TET2, and TET3. Previous research suggests that DNMT3L interacts with DNMT3A/B to facilitate methylation²⁷, whereas proteins of the TET family exert an opposing effect^{28,29}. Consequently, we hypothesize that the reduced methylation level of hnRNPA3 may be modulated by DNMT3L, TET1, TET2, and TET3.

MiRNAs are a class of small non-coding RNAs encoded by endogenous genes and are approximately 23 nucleotides in length¹⁰. miRNAs are involved in the post-transcriptional regulation of genes and are widely present and play an important role in animals and plants, and can participate in the regulation of cell growth, differentiation, development, apoptosis, and other activities³⁰. According to reports, miR-22-3p plays as a tumor suppressor in several cancers. In NSCLC, miR-22-3p suppresses cell migration and EMT via targeting RAC1 expression³¹. Down-regulation of miR-22-3p promotes the progression and poor prognosis of cervical cancer³². Cell Proliferation and migration of Gastric Cancer suppressed by miR-22-3p by Targeting ENO1³³. There are also several evidences have reported the function and potential mechanisms of miR-22-3p in HCC. Catalpol inhibits cell proliferation, invasion and migration through regulating miR-22-3p/MTA3 signalling in hepatocellular carcinoma³⁴. targeting Sp1, Berberine upregulates miR-22-3p to suppress HCC proliferation³⁵. Interestingly, Chen et al³⁶ reported miR-22-3p was associated with HCC cells stemness, growth, and metastasis directly targeting TET2. As we said, TET2 is a methyltransferase to demethylate DNA. We noticed These results were in line with the above conclusion that hnRNPA3 related to DNA methylation. So, we speculated that hnRNPA3 may be a significant biomarker in HCC regulated by miR-22-3p and DNA methylation.

Spatial transcriptomics is a recently emerged technology that integrates sequencing data with spatial localization, offering a unique perspective for studying the tumor immune microenvironment distinct from conventional transcriptomic sequencing³⁷. In this study, we initially employed TIMER to quantify the immune cell composition within the TCGA-LIHC transcriptomic dataset, uncovering a significant correlation between hnRNPA3 expression and macrophages. To corroborate this finding, we investigated spatial transcriptomic sequencing data, which yielded concordant results, indicating a spatial as well as transcriptomic intimacy between hnRNPA3 and macrophages. In idiopathic pulmonary arterial hypertension (IPAH), it has been suggested that hnRNPA3 may participate in the pathogenesis by modulating macrophage polarization states, aligning with our current observations³⁸.

Chemotherapy and targeted therapy are the primary modalities for the treatment of HCC. So making the exploration of chemotherapeutic and targeted therapeutic drug sensitivity is an urgent issue. In this study, by integrating the pRRophetic package with the expression level of hnRNPA3, we predicted that the IC50 values for drugs such as 5-fluorouracil, Doxorubicin, and Etoposide were significantly reduced in the high hnRNPA3 expression group. Consequently, we hypothesize that hnRNPA3 may be involved in regulating the mechanisms of action of these drugs in HCC. Transcriptomic sequencing results from cell

lines in this study suggest that hnRNPA3 may participate in the regulation of the PI3K/AKT pathway. Interestingly, previous studies have reported that 5-fluorouracil (5-FU), Doxorubicin, and Etoposide are involved in the regulation of the PI3K-AKT pathway³⁹⁻⁴¹. Therefore, we speculate that hnRNPA3 may modulate the resistance to 5-fluorouracil, Doxorubicin, and Etoposide through the PI3K-AKT pathway, which warrants further validation and investigation.

Rapid proliferation and metastasis are major features of HCC. We performed a series of experiments in vitro. CCK-8 and colony formation assays revealed that low expression of HNRNPA3 suppressed cells proliferation. The transwell and scratch assays showed the hnRNPA3 promoted tumors migration. RNA-seq and enrichment analysis also underscored that the DEGs were enriched in the Rap1, MAPK and PI3K-Akt signaling pathway, and biological processes like cell adhesion, signal transduction, and the regulation of cell proliferation.

Conclusion

In summary, we screened the tumor promoter hnRNPA3 through combined datasets analysis and verified that hnRNPA3 could promote HCC proliferation and metastasis in vitro. As an epigenic modification related gene, hnRNPA3 could be regulated by modulating the DNA methylation status and ceRNA to influence HCC immunoinfiltration and result in tumors malignant progression. To sum up, hnRNPA3 was found to represent a promising biomarker within HCC diagnosis and prognosis and maybe a potential drug-target in HCC therapy.

Declarations

Funding

This project was supported by Hangzhou Medical College Basic Scientific Research Fund - Youth Fund (KYQN202120) and The Medicine and Health Research Foundation of Zhejiang Province(2024636793 and 2024KY770)

Ethics and Consent to Participate

Not applicable

Author contribution

Conceived and designed the experiments: Guangyuan Song, Zhenyuan Qian

Analyzed the data: Weihui Guo, Fang Wu, Tao Ding, Yizhe Diao

Wrote and revised the paper: Xufan Cai, Weihui Guo, Yizhe Diao

Draw figures: Weihui Guo, Wei Lang Xu, Lei Wang

Conflict of interest

The authors declared no competing interests.

Acknowledgement

We sincerely thanks Doc. Yang Xu (Department of Thoracic Surgery, Zhejiang Cancer Hospital, Zhejiang China) for his guidance and help in bioinformatics

Consent for publications

Not applicable

References

1. Sung H, Ferlay J, Siegel RL, Laversanne M, Soerjomataram I, Jemal A, Bray F. Global Cancer Statistics 2020: GLOBOCAN Estimates of Incidence and Mortality Worldwide for 36 Cancers in 185 Countries. *CA Cancer J Clin.* 2021;71(3):209–49. <https://doi.org/10.3322/caac.21660>.
2. Kędzierska H, Piekietko-Witkowska A. Splicing Factors of SR and hnRNP Families as Regulators of Apoptosis in Cancer. *Cancer Lett.* 2017;396:53–65. <https://doi.org/10.1016/j.canlet.2017.03.013>.
3. Geuens T, Bouhy D, Timmerman V. The hnRNP Family: Insights into Their Role in Health and Disease. *Hum Genet.* 2016;135(8):851–67. <https://doi.org/10.1007/s00439-016-1683-5>.
4. Kim D, Pertea G, Trapnell C, Pimentel H, Kelley R, Salzberg SL. TopHat2: Accurate Alignment of Transcriptomes in the Presence of Insertions, Deletions and Gene Fusions. *Genome Biol.* 2013;14(4):R36. <https://doi.org/10.1186/gb-2013-14-4-r36>.
5. Boukakis G, Patrinoiu-Georgoula M, Lekarakou M, Valavanis C, Guialis A. Deregulated Expression of hnRNP A/B Proteins in Human Non-Small Cell Lung Cancer: Parallel Assessment of Protein and mRNA Levels in Paired Tumour/Non-Tumour Tissues. *BMC Cancer.* 2010;10(1):434. <https://doi.org/10.1186/1471-2407-10-434>.
6. Ren X, Dong Y, Duan M, Zhang H, Gao P. Abnormal Expression of HNRNPA3 in Multistep Hepatocarcinogenesis. *Oncol Lett.* 2021;21(1):46. <https://doi.org/10.3892/ol.2020.12307>.
7. Xu Z, Shi J, Chen Q, Yang S, Wang Z, Xiao B, Lai Z, Jin Y, Li Y, Li X. Regulation of de Novo and Maintenance DNA Methylation by DNA Methyltransferases in Post-Implantation Embryos. *J Biol Chem.* 2024;107990. <https://doi.org/10.1016/j.jbc.2024.107990>.
8. Smith ZD, Hetzel S, Meissner ADNA. Methylation in Mammalian Development and Disease. *Nat Rev Genet.* 2025;26(1):7–30. <https://doi.org/10.1038/s41576-024-00760-8>.
9. Liu Y, Xu Z, Shi J, Zhang Y, Yang S, Chen Q, Song C, Geng S, Li Q, Li J, Xu G-L, Xie W, Lin H, Li X. DNA Methyltransferases Are Complementary in Maintaining DNA Methylation in Embryonic Stem Cells. *iScience* 2022, 25 (9), 105003. <https://doi.org/10.1016/j.isci.2022.105003>

10. Bartel DP, MicroRNAs. Target Recognition and Regulatory Functions. *Cell*. 2009;136(2):215–33. <https://doi.org/10.1016/j.cell.2009.01.002>.
11. Gonzales LR, Blom S, Henriques R, Bachem CWB, Immink RGH, LncRNAs. The Art of Being Influential without Protein. *Trends Plant Sci*. 2024;29(7):770–85. <https://doi.org/10.1016/j.tplants.2024.01.006>.
12. Li T, Fu J, Zeng Z, Cohen D, Li J, Chen Q, Li B, Liu XS. TIMER2.0 for Analysis of Tumor-Infiltrating Immune Cells. *Nucleic Acids Res*. 2020;48(W1):W509–14. <https://doi.org/10.1093/nar/gkaa407>.
13. Xu L, Deng C, Pang B, Zhang X, Liu W, Liao G, Yuan H, Cheng P, Li F, Long Z, Yan M, Zhao T, Xiao Y, Li XTIP. A Web Server for Resolving Tumor Immunophenotype Profiling. *Cancer Res*. 2018;78(23):6575–80. <https://doi.org/10.1158/0008-5472.CAN-18-0689>.
14. Xun Z, Ding X, Zhang Y, Zhang B, Lai S, Zou D, Zheng J, Chen G, Su B, Han L, Ye Y. Reconstruction of the Tumor Spatial Microenvironment along the Malignant-Boundary-Nonmalignant Axis. *Nat Commun*. 2023;14(1):933. <https://doi.org/10.1038/s41467-023-36560-7>.
15. Hao Y, Hao S, Andersen-Nissen E, Mauck WM, Zheng S, Butler A, Lee MJ, Wilk AJ, Darby C, Zager M, Hoffman P, Stoeckius M, Papalexi E, Mimitou EP, Jain J, Srivastava A, Stuart T, Fleming LM, Yeung B, Rogers AJ, McElrath JM, Blish CA, Gottardo R, Smibert P, Satija R. *Cell*. 2021;184(13):3573–e358729. <https://doi.org/10.1016/j.cell.2021.04.048>. Integrated Analysis of Multimodal Single-Cell Data.
16. Geeleher P, Cox N, Huang RS, pRRophetic. An R Package for Prediction of Clinical Chemotherapeutic Response from Tumor Gene Expression Levels. *PLoS ONE*. 2014;9(9):e107468. <https://doi.org/10.1371/journal.pone.0107468>.
17. Fakan S, Leser G, Martin TE. Ultrastructural Distribution of Nuclear Ribonucleoproteins as Visualized by Immunocytochemistry on Thin Sections. *J Cell Biol*. 1984;98(1):358–63. <https://doi.org/10.1083/jcb.98.1.358>.
18. Tanaka E, Fukuda H, Nakashima K, Tsuchiya N, Seimiya H, Nakagama H. HnRNP A3 Binds to and Protects Mammalian Telomeric Repeats in Vitro. *Biochem Biophys Res Commun*. 2007;358(2):608–14. <https://doi.org/10.1016/j.bbrc.2007.04.177>.
19. Guo NL, Wan Y-W, Tosun K, Lin H, Msiska Z, Flynn DC, Remick SC, Vallyathan V, Dowlati A, Shi X, Castranova V, Beer DG, Qian Y. Confirmation of Gene Expression-Based Prediction of Survival in Non-Small Cell Lung Cancer. *Clin Cancer Res*. 2008;14(24):8213–20. <https://doi.org/10.1158/1078-0432.CCR-08-0095>.
20. Guo L, Ma Y, Ward R, Castranova V, Shi X, Qian Y. Constructing Molecular Classifiers for the Accurate Prognosis of Lung Adenocarcinoma. *Clin Cancer Res*. 2006;12(11 Pt 1):3344–54. <https://doi.org/10.1158/1078-0432.CCR-05-2336>.
21. Xing S, Wang Y, Hu K, Wang F, Sun T, Li QWGCNA. Reveals Key Gene Modules Regulated by the Combined Treatment of Colon Cancer with PHY906 and CPT11. *Biosci Rep*. 2020;40(9). <https://doi.org/10.1042/BSR20200935>.

22. Taoka Y, Matsumoto K, Ohashi K, Minamida S, Hagiwara M, Nagi S, Saito T, Kodera Y, Iwamura M. Protein Expression Profile Related to Cisplatin Resistance in Bladder Cancer Cell Lines Detected by Two-Dimensional Gel Electrophoresis. *Biomed Res.* 2015;36(4):253–61. <https://doi.org/10.2220/biomedres.36.253>.
23. Koch A, Joosten SC, Feng Z, De Ruijter TC, Draht MX, Melotte V, Smits KM, Veeck J, Herman JG, Van Neste L, Van Criekinge W, De Meyer T, Van Engeland M. Analysis of DNA Methylation in Cancer: Location Revisited. *Nat Rev Clin Oncol.* 2018;15(7):459–66. <https://doi.org/10.1038/s41571-018-0004-4>.
24. Long J, Chen P, Lin J, Bai Y, Yang X, Bian J, Lin Y, Wang D, Yang X, Zheng Y, Sang X, Zhao HDNA. Methylation-Driven Genes for Constructing Diagnostic, Prognostic, and Recurrence Models for Hepatocellular Carcinoma. *Theranostics.* 2019;9(24):7251–67. <https://doi.org/10.7150/thno.31155>.
25. Klutstein M, Nejman D, Greenfield R, Cedar H. DNA Methylation in Cancer and Aging. *Cancer Res.* 2016;76(12):3446–50. <https://doi.org/10.1158/0008-5472.CAN-15-3278>.
26. Morgan AE, Davies TJ, Mc Auley MT. The Role of DNA Methylation in Ageing and Cancer. *Proc. Nutr. Soc.* 2018, 77(4), 412–422. <https://doi.org/10.1017/S0029665118000150>
27. A E-O. DNMT Cooperativity—the Developing Links between Methylation, Chromatin Structure and Cancer. *BioEssays: news reviews Mol Cell Dev biology.* 2003;25(11). <https://doi.org/10.1002/bies.10345>.
28. If L-M, M K, Pg H, A R. TET Enzymes in the Immune System: From DNA Demethylation to Immunotherapy, Inflammation, and Cancer. *Annu Rev Immunol.* 2024;42(1). <https://doi.org/10.1146/annurev-immunol-080223-044610>.
29. Kd R, K H. Role of TET Enzymes in DNA Methylation, Development, and Cancer. *Genes Dev.* 2016;30(7). <https://doi.org/10.1101/gad.276568.115>.
30. Saliminejad K, Khorram Khorshid HR, Soleymani Fard S, Ghaffari SH. An Overview of microRNAs: Biology, Functions, Therapeutics, and Analysis Methods. *J Cell Physiol.* 2019;234(5):5451–65. <https://doi.org/10.1002/jcp.27486>.
31. Wang X, Wang X, Jiang T, Zhang Z, Xie N, Yang G. MiR-22-3p Suppresses NSCLC Cell Migration and EMT via Targeting RAC1 Expression. *Funct Integr Genomics.* 2023;23(3):281. <https://doi.org/10.1007/s10142-023-01211-z>.
32. Kwon A-Y, Jeong J-Y, Park H, Hwang S, Kim G, Kang H, Heo J-H, Lee HJ, Kim T-H, An HJ. miR-22-3p and miR-30e-5p Are Associated with Prognosis in Cervical Squamous Cell Carcinoma. *Int J Mol Sci.* 2022;23(10):5623. <https://doi.org/10.3390/ijms23105623>.
33. Qiao H, Wang N, Guan Q-L, Xie P, Li X-K. miR-22-3p Suppresses Cell Proliferation and Migration of Gastric Cancer by Targeting ENO1. *Altern Ther Health Med.* 2023;29(5):278–83.
34. Zhao L, Wang Y, Liu Q. Catalpol Inhibits Cell Proliferation, Invasion and Migration through Regulating miR-22-3p/MTA3 Signalling in Hepatocellular Carcinoma. *Exp Mol Pathol.* 2019;109:51–60. <https://doi.org/10.1016/j.yexmp.2019.104265>.

35. Chen J, Wu F-X, Luo H-L, Liu J-J, Luo T, Bai T, Li L-Q, Fan X-H. Berberine Upregulates miR-22-3p to Suppress Hepatocellular Carcinoma Cell Proliferation by Targeting Sp1. *Am J Transl Res*. 2016;8(11):4932–41.
36. Chen D, Yan Y, Wang X, Li S, Liu Y, Yu D, He Y, Deng R, Liu Y, Xu M, Luo J, Gao H, Wang S. Chronic Alcohol Exposure Promotes HCC Stemness and Metastasis through β -Catenin/miR-22-3p/TET2 Axis. *Aging (Milano)*. 2021;13(10):14433–55. <https://doi.org/10.18632/aging.203059>.
37. Liu Y, Xun Z, Ma K, Liang S, Li X, Zhou S, Sun L, Liu Y, Du Y, Guo X, Cui T, Zhou H, Wang J, Yin D, Song R, Zhang S, Cai W, Meng F, Guo H, Zhang B, Yang D, Bao R, Hu Q, Wang J, Ye Y, Liu L. Identification of a Tumour Immune Barrier in the HCC Microenvironment That Determines the Efficacy of Immunotherapy. *J Hepatol*. 2023;78(4):770–82. <https://doi.org/10.1016/j.jhep.2023.01.011>.
38. Wei R, Chen L, Li P, Lin C, Zeng Q. IL-13 Alleviates Idiopathic Pulmonary Hypertension by Inhibiting the Proliferation of Pulmonary Artery Smooth Muscle Cells and Regulating Macrophage Infiltration. *Am J Transl Res*. 2022;14(7):4573–90.
39. Zhang W, Ding W, Chen Y, Feng M, Ouyang Y, Yu Y, He Z. Up-Regulation of Breast Cancer Resistance Protein Plays a Role in HER2-Mediated Chemoresistance through PI3K/Akt and Nuclear Factor-Kappa B Signaling Pathways in MCF7 Breast Cancer Cells. *Acta Biochim Biophys Sin (Shanghai)*. 2011;43(8):647–53. <https://doi.org/10.1093/abbs/gmr050>.
40. Wang L, Liu Y, Li S, Zha Z, Chen Y, Wang Q, Zhou S, Huang X, Xu M. Capsaicin Alleviates Doxorubicin-Induced Acute Myocardial Injury by Regulating Iron Homeostasis and PI3K-Akt Signaling Pathway. *Aging*. 2023;15(21):11845–59. <https://doi.org/10.18632/aging.205138>.
41. Zhang J, Zhao H, Feng Y, Xu X, Yang Y, Zhang P, Lu Z, Zhang T. Topoisomerase 2 Inhibitor Etoposide Promotes Interleukin-10 Production in LPS-Induced Macrophages via Upregulating Transcription Factor Maf and Activating PI3K/Akt Pathway. *Int Immunopharmacol* 2021, 101 (Pt A), 108264. <https://doi.org/10.1016/j.intimp.2021.108264>

Figures

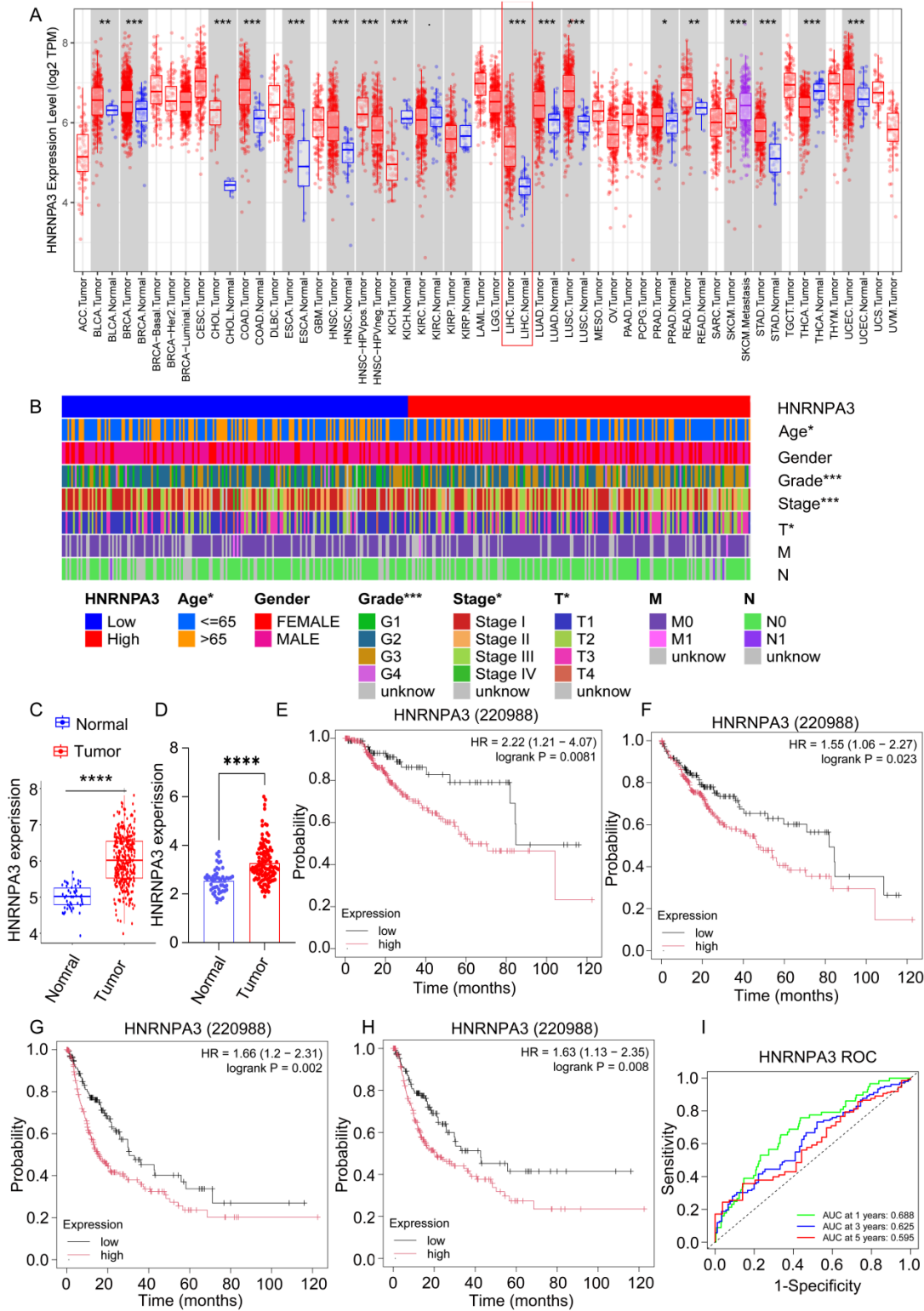


Figure 1

HNRNPA3 Expression Analysis.

A. hnRNP3 expression in cancer and normal tissues in pan-cancer TCGA dataset. B. The relationship between hnRNP3 and HCC clinicopathological features. C. hnRNP3 expression in HCC tumors and normal tissues from TCGA and GEO. (D, E, F, G). hnRNP3 expression was correlated with worse

prognosis of HCC (DFS, OS, PFS, RFS). H. The prognostic capacity of HNRNPA3 was evaluated by using the AUC at 1-,3- and 5-year of ROC curves.

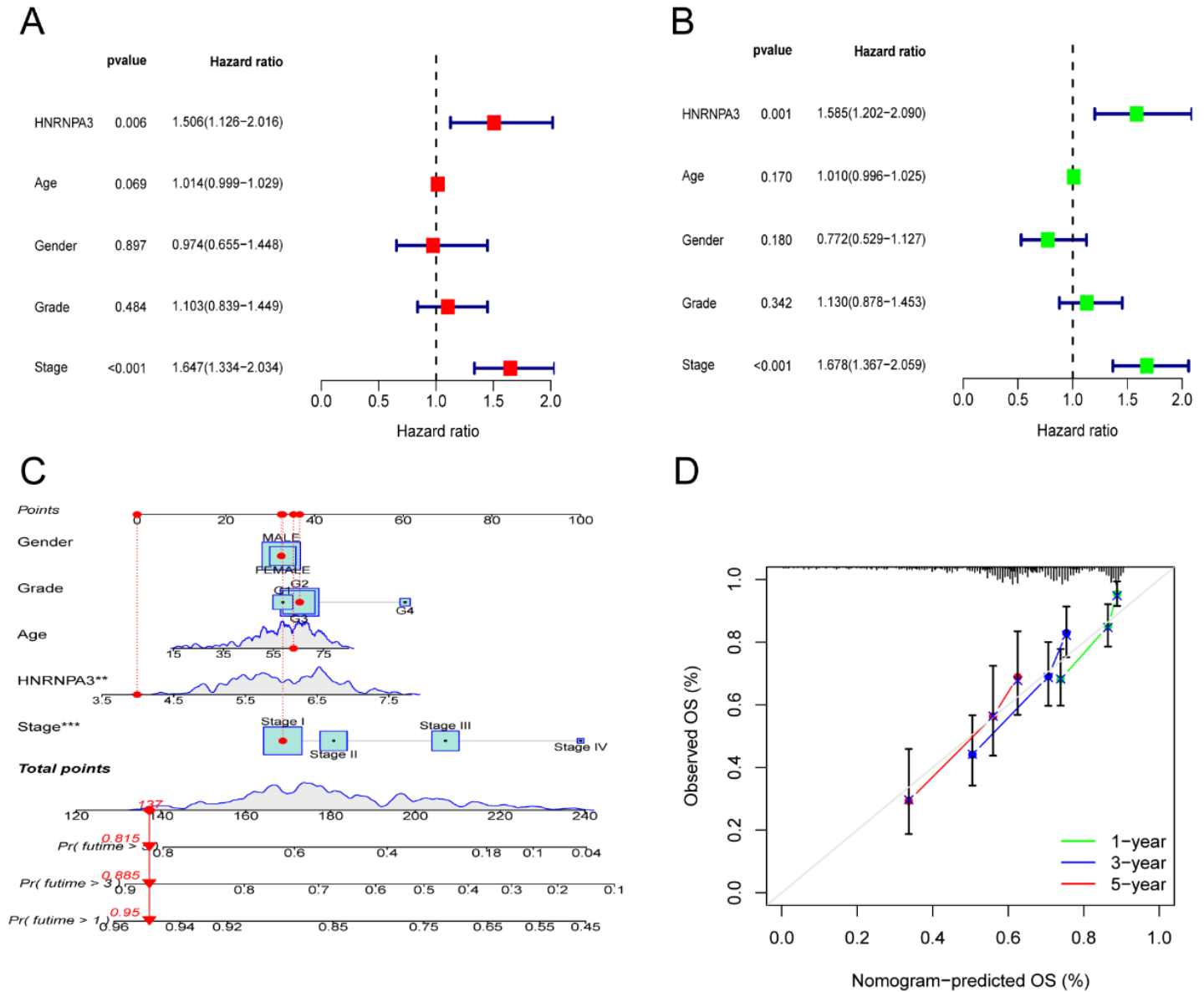


Figure 2

Prognostic prediction model of HNRNPA3 in LIHC.

A. Univariate Cox regression visualization by the forest plot. B. multivariate Cox regression visualization by the forest plot. C. Nomogram for 1-, 3-, and 5-year OS of patients with LIHC. D. The calibration plots for predicting OS at 1-, 3-, and 5-year.

stages. E. Survival curves of cg11064170 on DFI in HCC. F. Survival curves of cg11064170 on OS in HCC. G. Survival curves of cg01594915 on OS in HCC. H. Survival curves of cg01750051 on DFI in HCC. (I, J K, L). Correlation between SNHG16 and DNMT3L, TET1, TET2, and TET3 in HCC. (M, N, O, P). Overall survival curves of hnRNPA3 combined with DNMT3L, TET1, TET2, or TET3 in HCC.

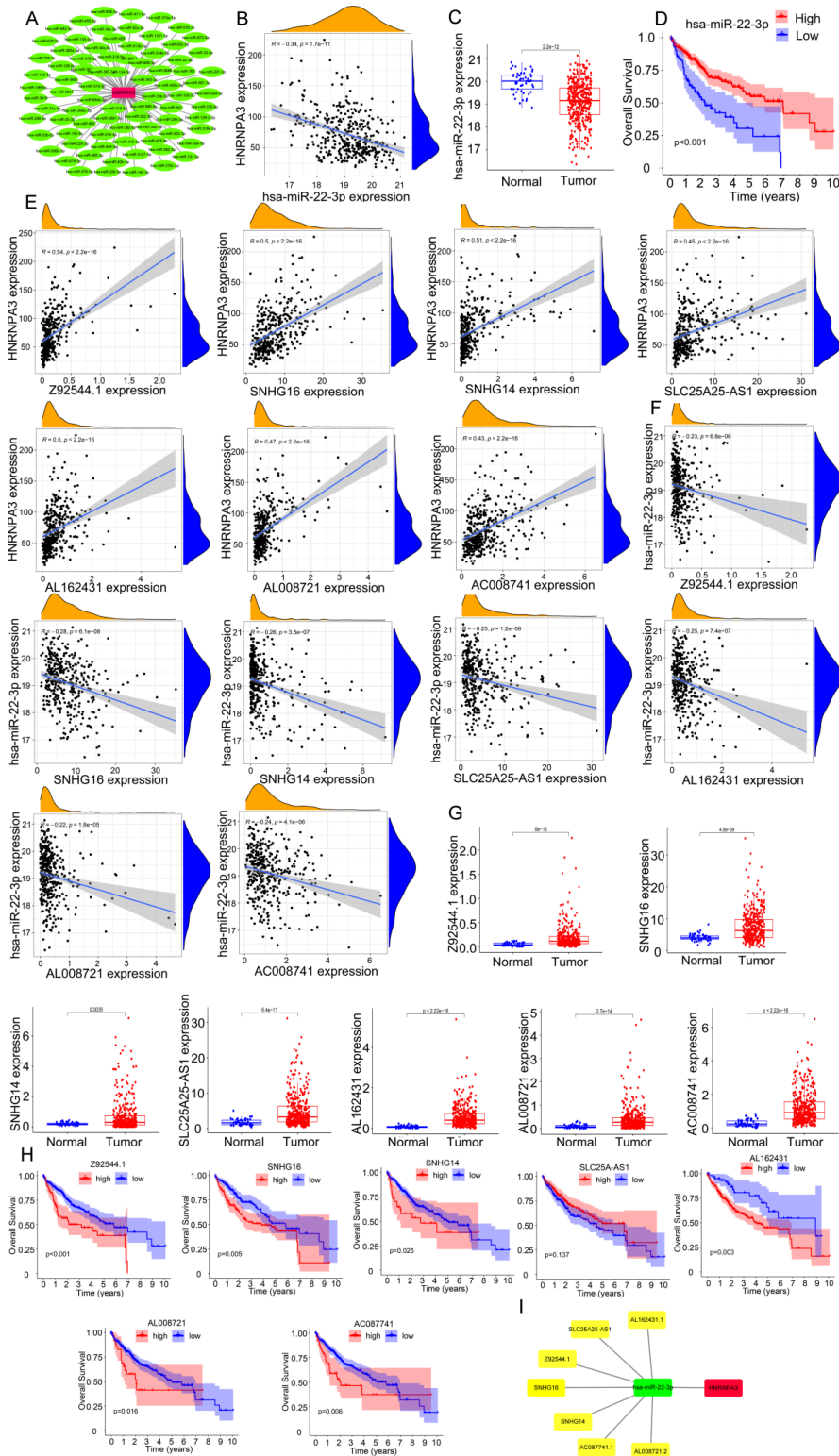


Figure 4

ceRNA network of hnRNPA3.

A. The miRNA-HNRNPA3 interaction network. B. Correlation plot between hsa-miR-22-3p and hnRNP A3. C. The expression level of hsa-miR-22-3p between tumors and normal tissues. D. Overall survival curves of hsa-miR-22-3p in HCC. E. LncRNAs positively correlated with hnRNP A3 in HCC. F. LncRNAs negatively correlated with hnRNP A3 in HCC. G. LncRNAs positively correlated with hnRNP A3 in cancer and normal tissues expression levels. H. Survival curve plot of positively correlated LncRNAs in LIHC. I. ceRNA network of hnRNP A3 in HCC.

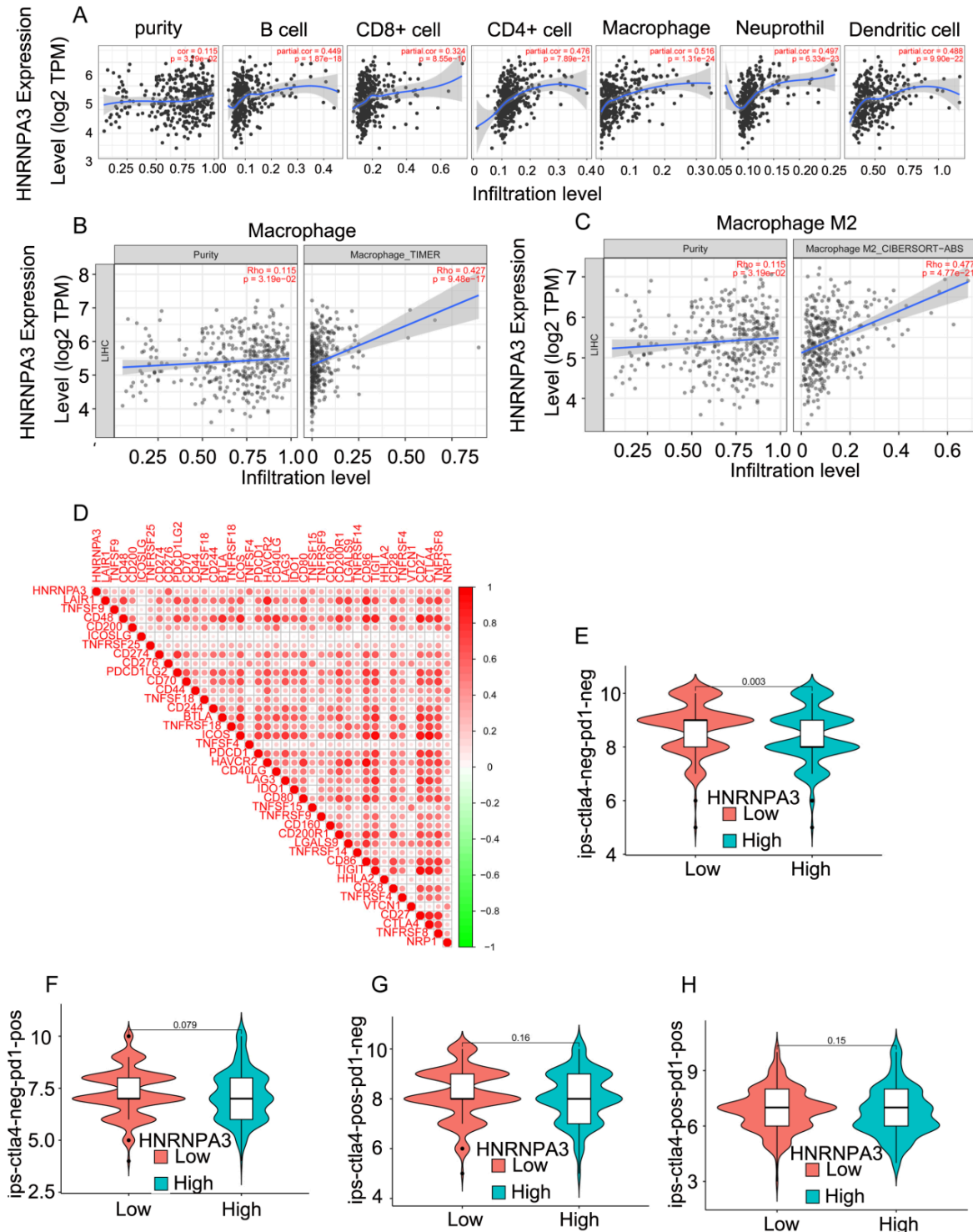


Figure 5

hnRNPA3 expression and immune infiltration.

A. Correlation between hnRNPA3 expression and the relative abundances of 6 immune cells from TIMER datasets. (B, C, D). Correlation between hnRNPA3 and macrophages form TIMER dataset. (E, F, G, H). The immune responsiveness of the groups was evaluated through IPS evaluation .

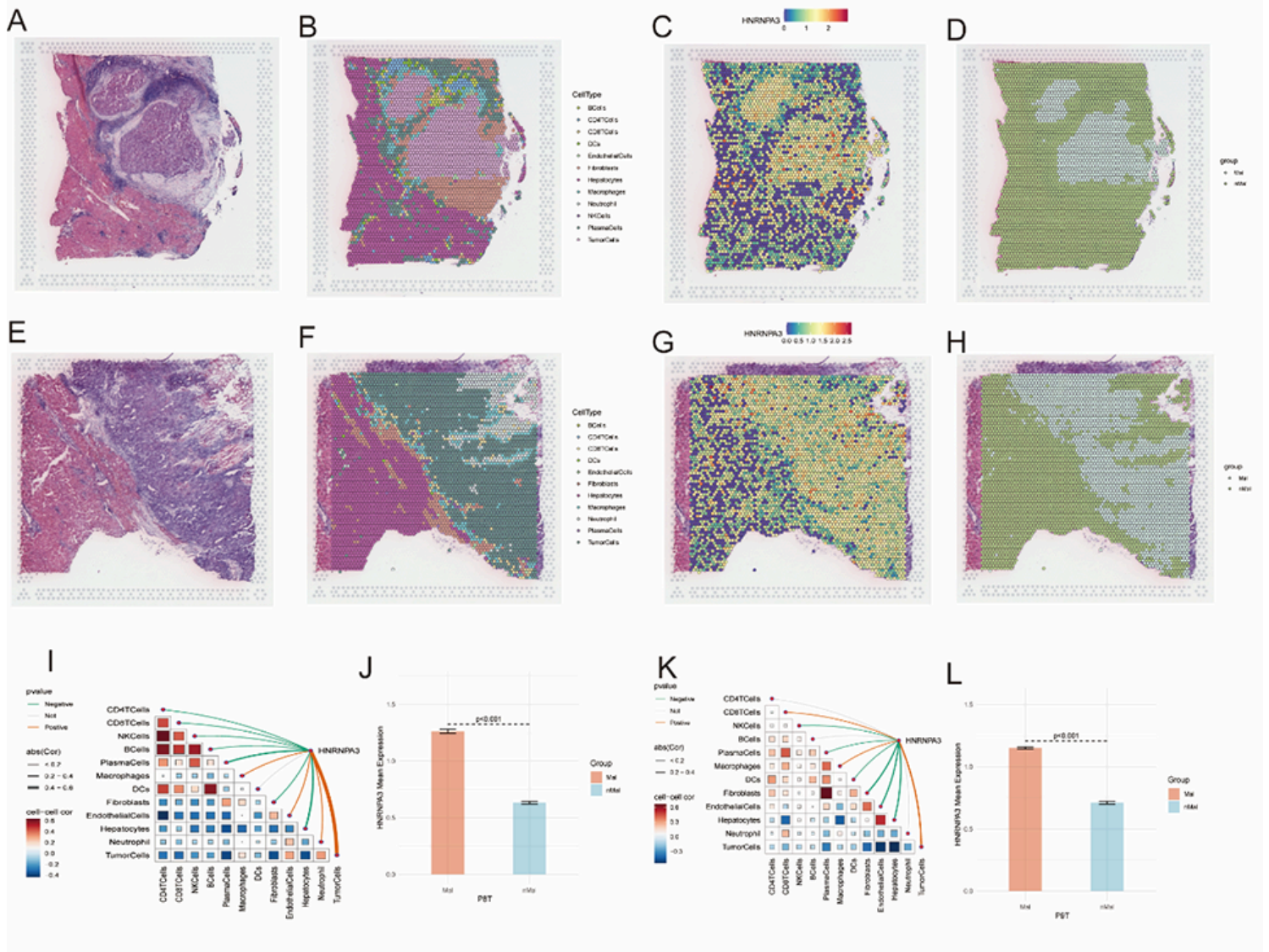


Figure 6

Spatial transcriptomics analysis revealing hnRNPA3 in LIHC.

(A, B, C, D). Expression and localization of 12 types of immune-related cells, hnRNPA3, and malignant cells in P8T. (E, F, G, H). Expression and localization of 12 types of immune-related cells, hnRNPA3, and malignant cells in P9T. I. The correlation between hnRNPA3 and the content of 12 types of immune cells in P8T. J. The difference of hnRNPA3 between the malignant cell group (Mal) and the non-malignant cell group (nMal) in P8T. K. The correlation between hnRNPA3 and the content of 12 types of immune cells in P9T. L. The difference of hnRNPA3 between the malignant cell group (Mal) and the non-malignant cell group (nMal) in P9T.

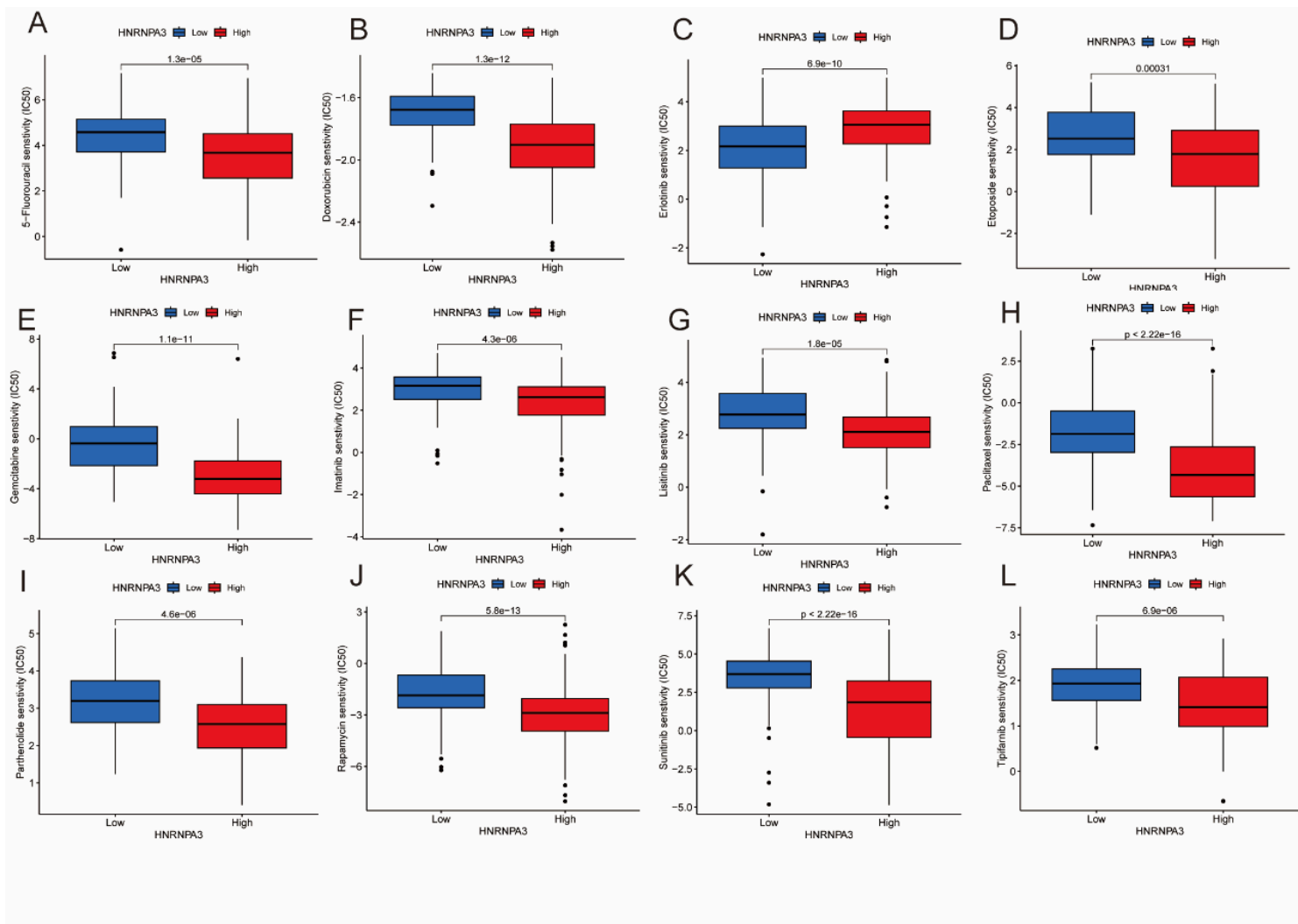


Figure 7

The relationship between drug sensitivity prediction and HNRNPA3.

(A,B,C,D,E,F,G,H,I,J). The IC50 differences of 12 drugs between high hnRNPA3 expression and low HNRNPA3 expression.

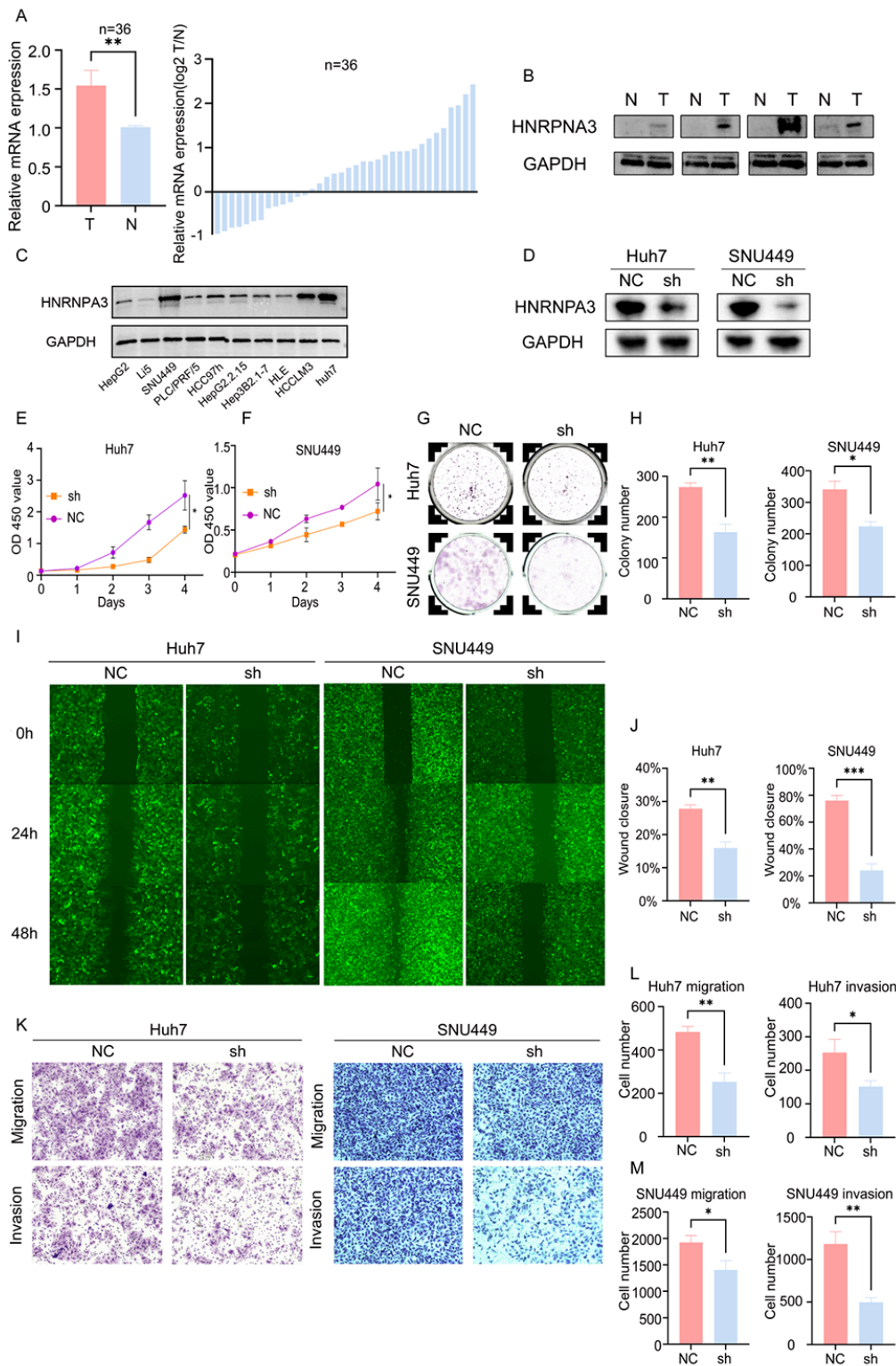


Figure 8

The role of hnRNPA3 in HCC

A. qRT-PCR to detect the mRNA expression of hnRNPA3 between tumors and normal tissues(n=36). B. using WB to detect the protein expression of hnRNPA3 in several paired samples. C.comparing hnRNPA3 expression in 9 HCC cell lines and Li5 cell lines. D. The efficiency of silenced hnRNPA3 verified by WB. (E,

F). CCK-8 revealed the growth trend of HCC cells after knockdown of hnRNPA3. (G, H). Effect of knocking down hnRNPA3 on the proliferation of cells by colony formation assay. (I, J). cell migration capacity detected by scratch test. (K, L, M). Cell migration regulation capacity by transwell assays after hnRNPA3 knockdown. *, P<0.05; **, P<0.01; ***, P<0.001.

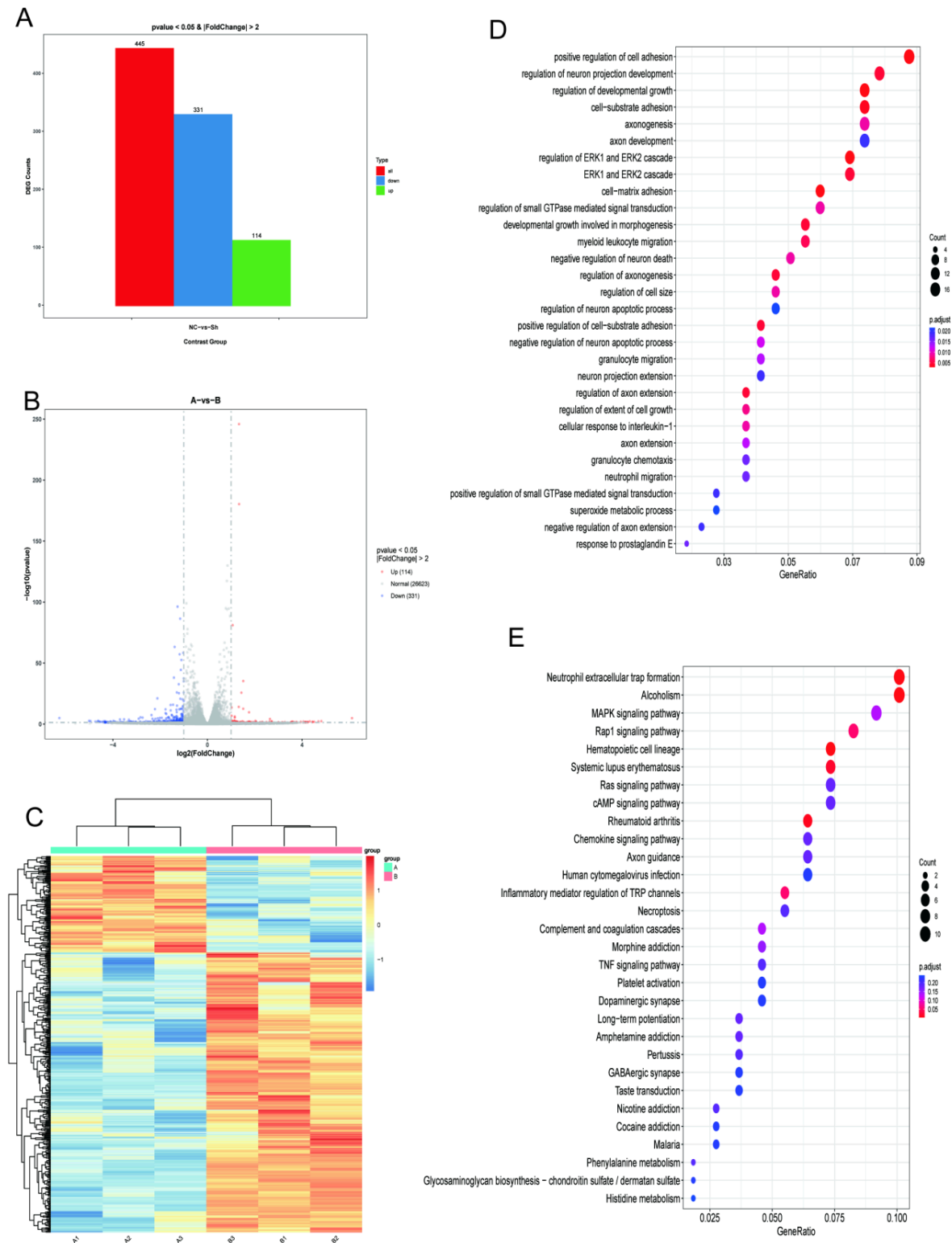


Figure 9

mRNA sequencing showed the role of hnRNPA3 in transcriptional programs of HCC.

A. DEGs histogram. B. DEGs volcano plot. C. DEGs heatmap. D. GO enrichment analysis. E. KEGG enrichment analysis.